

## Optical Stark Effects in *J*-Aggregate–Metal Hybrid Nanostructures Exhibiting a Strong Exciton–Surface-Plasmon-Polariton Interaction

P. Vasa,<sup>1,2,\*</sup> W. Wang,<sup>1</sup> R. Pomraenke,<sup>1</sup> M. Maiuri,<sup>3</sup> C. Manzoni,<sup>3</sup> G. Cerullo,<sup>3</sup> and C. Lienau<sup>1,†</sup>

<sup>1</sup>*Institut für Physik, Carl von Ossietzky Universität, D-26111 Oldenburg, Germany*

<sup>2</sup>*Department of Physics, Indian Institute of Technology Bombay, 400076 Mumbai, India*

<sup>3</sup>*IFN-CNR, Dipartimento di Fisica, Politecnico di Milano, 20133 Milano, Italy*

(Received 10 June 2014; published 21 January 2015)

We report on the observation of optical Stark effects in *J*-aggregate–metal hybrid nanostructures exhibiting strong exciton-surface-plasmon-polariton coupling. For redshifted nonresonant excitation, pump-probe spectra show short-lived dispersive line shapes of the exciton-surface-plasmon-polariton coupled modes caused by a pump-induced Stark shift of the polariton resonances. For larger coupling strengths, the sign of the Stark shift is reversed by a transient reduction in normal mode splitting. Our studies demonstrate an approach to coherently control and largely enhance optical Stark effects in strongly coupled hybrid systems. This may be useful for applications in ultrafast all-optical switching.

DOI: 10.1103/PhysRevLett.114.036802

PACS numbers: 73.20.Mf, 71.70.Ej, 72.80.Le, 78.47.J-

The optical Stark effect (OSE) is a fundamental, coherent nonlinear interaction involving transient shifts of energy levels in the presence of a nonresonant light field [1–3]. Being a coherent interaction, it is promising for implementing quantum information processing [4,5]. It has been demonstrated in atoms [1,2] and semiconductor nanostructures [6–11]. In some systems, it can be satisfactorily described by a two-level system interacting with a coherent, transient light field [1,8]. In others, e.g., semiconductor quantum wells, many-body interactions prevail [12,13], strongly influencing the OSE. Its study therefore can provide important insights into the quantum dynamics of optical excitations.

Molecular aggregates [14] have recently received considerable interest [15–17]. Because of their large optical dipole moment they serve as prototypes for exploring dipolar coupling between excitons (Xs) and surface plasmon polaritons (SPPs). Strong X-SPP coupling and the formation of hybrid polariton modes has now been demonstrated [16,18–24] and normal mode splitting up to ~700 meV has been achieved [23]. This makes them attractive for implementing active-photonic functionalities like ultrafast optical switching [16,21–23,25–27], signal processing, and lasing at the nanoscale [28,29]. So far, X-SPP polariton switching has been explored either under nonresonant excitation, yielding a comparatively slow, incoherent response [22,25], or it demands challenging resonant excitation [16]. Off-resonant, coherent control of the coupled X-SPP modes by the OSE might provide fundamental insight into the quantum dynamics of hybrid systems. Despite its obvious potential, it has not been demonstrated yet to the best of our knowledge.

We report in this Letter the first experimental observation of OSEs in *J*-aggregate–metal hybrid nanostructures exhibiting strong X-SPP coupling. For hybrid systems with

moderate normal mode splitting, we observe the expected transient light-induced dressing [2,6,8–10] of the polaritons. For larger normal mode splitting, however, the pump-induced coherent exciton population transiently reduces the X-SPP coupling [16,22,25], resulting in a sign reversal and significant enhancement of the OSE. Such a coherent all-optical nonlinearity may be interesting for implementing all-optical switching.

We investigate hybrid nanostructures consisting of a ~50 nm thick *J*-aggregated cyanine dye (2,2'-dimethyl-8-phenyl-5,6,5',6'-dibenzothiacarbocyanine chloride, Hayashibara Biochemicals Laboratories, Inc.) layer spin coated onto a periodic nanogroove array with a 400 nm period in a gold film [16,22,24,30]. We have recorded *p*-polarized linear reflectivity spectra  $R_0(\omega_{pr})$  and differential reflectivity maps  $\Delta R/R(\tau, \omega_{pr}) = (R_{on} - R)/R$ . Here  $\omega_{pr}$  is the probe frequency and  $R_{on}$  ( $R$ ) is the reflected probe pulse spectrum in the presence (absence) of the pump pulse, recorded as a function of the delay  $\tau$  between pump and probe pulses [16,30,46]. The differential reflectivity setup uses a noncollinear optical parametric amplifier generating broadband pulses centered at 1.8 eV and having 1.65–1.9 eV extent. The pump spectrum is narrowed by a bandpass filter centered at 1.75 eV with a 24 meV linewidth, whereas the probe pulses are broadband. Typical pump (probe) pulse fluence used in these experiments is 90  $\mu\text{J}/\text{cm}^2$  (6  $\mu\text{J}/\text{cm}^2$ ). All experiments are performed at room temperature under vacuum to minimize *J*-aggregate photobleaching.

The linear optical response [16,19–24] of such hybrid nanostructures is governed by the coupling of excitonic transition dipole moments to vacuum fluctuations of the groove array SPP modes. Because of this coupling, the isolated *J*-aggregate and SPP resonances are transformed into strongly coupled higher (UP) and lower energy (LP)

$X$ -SPP polariton modes, exhibiting a characteristic anticrossing with a normal mode splitting,  $|\Omega_{\text{NMS}}| \sim 60\text{--}110$  meV in our samples [20,30]. The linear optical properties of the coupled system are well explained [24,47–49] as those of the two complex Lorentzian oscillators representing the individual  $X$  and SPP systems, interacting via a dipole coupling,  $\Omega_{\text{NMS}} = 2 \int \boldsymbol{\mu}_{\text{eff}}(\mathbf{r}) \cdot \mathbf{E}_P(\mathbf{r}) d^3r$ . Here,  $\boldsymbol{\mu}_{\text{eff}} \propto \sqrt{N}$  denotes an effective dipole moment density and  $N$  is the exciton number.  $\mathbf{E}_P(\mathbf{r})$  gives the average strength of the local SPP vacuum electric field fluctuations at position  $\mathbf{r}$  [24]. The polariton eigenfrequencies obtained by diagonalizing the Hamiltonian matrix are given by

$$\tilde{\omega}_{\text{UP,LP}} = \frac{(\tilde{\omega}_X + \tilde{\omega}_P)}{2} \pm \frac{1}{2} \sqrt{(\tilde{\omega}_X - \tilde{\omega}_P)^2 + \Omega_{\text{NMS}}^2}, \quad (1)$$

where  $\tilde{\omega}_{X,P} = \omega_{X,P} - i\gamma_{X,P}$  are the uncoupled  $X$  and SPP (complex) eigenfrequencies, respectively.

We commence by investigating the response of a  $J$ -aggregate film to an ultrafast off-resonant excitation, schematically shown in Fig. 1(a). A pump frequency  $\omega_{\text{pu}}$ , red detuned from the  $J$ -aggregate resonance by 40 meV, enhances the OSE while minimizing the spectral overlap. Our previous experiments have shown that the optical

properties of the hybrid nanostructures can be well understood by phenomenologically treating the  $J$ -aggregate as a three-level system [14,16,22] consisting of a ground state ( $|0\rangle$ ),  $X$  state ( $|X\rangle$ ) and biexciton state ( $|XX\rangle$ ). A weak, resonant probe pulse generates a coherent polarization in the two-level  $X$  system, which decays exponentially within the dephasing time. Under the dipole approximation and in the weak excitation limit, a delayed, redshifted pump pulse at  $\omega_{\text{pu}}$  and field  $E(t)$  forces the system to transiently oscillate at  $\omega_{\text{pu}}$ . This results in a blueshift of the transition frequency  $\tilde{\omega}_X$ , by an amount  $\Delta V(t) = \sqrt{(\tilde{\omega}_X - \omega_{\text{pu}})^2 + (\mu|E(t)|/\hbar)^2} + (\omega_{\text{pu}} - \tilde{\omega}_X)$ ,  $\mu$  being the effective  $X$  dipole moment [1,2,8]. The blueshift in turn generates a dispersive  $\Delta R$  line shape for pump delays within the excitonic dephasing time [8,30].

Measurements of the  $\Delta R/R(\tau, \omega_{\text{pr}})$  of a 50 nm thick  $J$ -aggregated film deposited on a flat gold mirror are reported in Fig. 1(b). They show an asymmetric dispersive response with a larger increase in reflectivity,  $\Delta R > 0$ , at the  $X$  resonance (1.79 eV) and a weaker reduction in reflectivity,  $\Delta R < 0$ , at a slightly higher probe frequency. The signal is observed only within  $\tau \sim \mp 70$  fs, much shorter than the  $X$  population relaxation time ( $\sim 0.5$  ps). Since the pump pulse duration is slightly longer than the  $X$  dephasing time [30], the signal mainly persists during the pulse overlap, supporting the assertion that the observed nonlinearity arises from an OSE.

To gain a more quantitative understanding, we performed optical Bloch equations (OBEs) simulations within the density matrix formalism [8,16,30] for the three-level scheme. An  $X$  population relaxation time of  $\sim 0.5$  ps, dephasing time of  $\sim 30$  fs, and transition dipole moment of 80 D ( $266.88 \times 10^{-30}$  C m) were assumed to satisfactorily describe the linear and nonlinear spectra [Fig. 1(c)] as well as  $\Delta R/R(\tau)$  [30]. The simulations suggest a transient blueshift of the  $X$  resonance  $\Delta V \sim 3$  meV [Fig. 1(d)]. The simulated pump-induced populations show weak  $XX$  population due to low excitation intensity [30], but the partial overlap between pump and  $X$  resonance results in a finite  $X$  population. Hence, the line shape of the nonlinear spectrum is given by the interplay between the OSE and saturation of  $X$  absorption. The latter results in a weak nonzero  $\Delta R/R$  signal at longer positive delays.

We now turn to the nonlinear response of the  $J$ -aggregate–metal hybrid nanostructures. It is recorded for a nanostructure with  $\Omega_{\text{NMS}} = 60$  meV with both pump and probe pulses incident at  $\theta = 29^\circ$ , close to the anti-crossing of the  $X$ -SPP polariton dispersion relation [30]. The excitation scheme and the recorded  $\Delta R/R(\tau, \omega_{\text{pr}})$  map are shown in Figs. 2(a) and 2(b). At  $\theta = 29^\circ$ , LP and UP resonances are observed at 1.78 and 1.9 eV, respectively. In our samples,  $X$ s are coupled to SPP excitations of a nanogroove array with fields concentrated near the grooves [16,22], whereas the  $J$ -aggregate molecules are

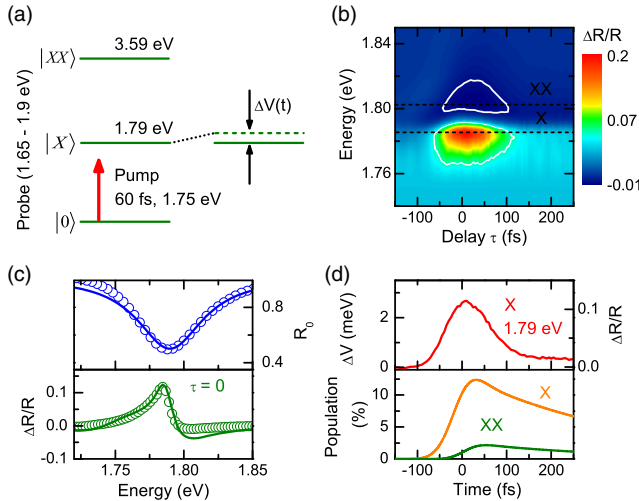


FIG. 1 (color online). (a) Schematic of the two-color pump-probe experiment performed on a  $J$ -aggregated dye layer. Narrow-band, 60 fs duration pump pulses at 1.75 eV non-resonantly excite the  $J$ -aggregate exciton transition ( $X$ ) at 1.79 eV. A broadband probe-pulse monitors the dynamics. The OSE results in a transient blueshift  $\Delta V(t)$  of the  $X$  transition. (b) The differential reflectivity map  $\Delta R/R(\omega_{\text{pr}}, \tau)$  shows a short-lived, asymmetric dispersive line shape at the  $X$  resonance arising from the interplay between the OSE and saturation of absorption. Dashed lines mark the maxima in  $\Delta R/R(\tau)$ . (c) Experimental (symbols) and simulated (line) linear (top) and zero-delay  $\Delta R/R$  (bottom) spectra. (d) Top: Stark shift  $\Delta V$  dynamics (left) deduced from the experimental  $\Delta R/R(\tau)$  (right). Bottom: simulated pump-induced  $X$  and biexciton ( $XX$ ) population dynamics.

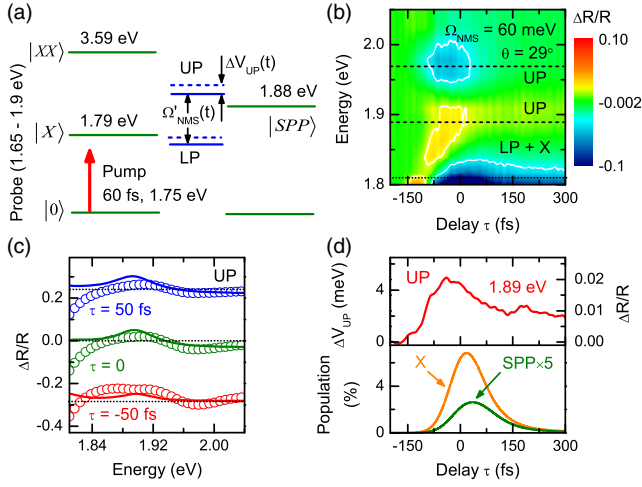


FIG. 2 (color online). (a) Schematic of the pump-probe experiment performed on a  $J$ -aggregate–metal nanostructure exhibiting strong  $X$ -SPP coupling. (b)  $\Delta R/R(\tau, \omega_{pr})$  map of a  $J$ -aggregate–metal hybrid structure with  $\Omega_{\text{NMS}} = 60$  meV recorded at  $\theta = 29^\circ$ , near the anticrossing. Dashed lines mark the maxima in  $\Delta R/R(\tau)$ . For pump pulses at 1.75 eV, the map shows a short-lived dispersive signal at the UP resonance (1.85–2.0 eV). (c) Experimental (symbols) and simulated (line)  $\Delta R/R$  spectra at selected delays. (d) Top: Stark shift  $\Delta V_{\text{UP}}$  dynamics (left) and  $\Delta R/R(\tau)$  (right) at the UP resonance. Bottom: calculated pump-induced  $X$  and SPP population dynamics.

uniformly distributed. Therefore, a large fraction of the  $X$ s remains uncoupled, resulting in a pronounced  $\Delta R$  signal near the  $X$  resonance. At  $\theta = 29^\circ$ , the nonlinear LP response overlaps with the uncoupled resonance (1.79 eV), making it difficult to separate the two contributions. Hence, we focus on the UP. Interestingly, it also shows a pronounced and dispersive  $\Delta R$  signal during pulse overlap, even though it is  $> 200$  meV blueshifted from  $\omega_{\text{pu}}$ .

For a strongly coupled system, the broadband probe pulse impulsively generates a coherent polarization at the two polariton frequencies. Under our excitation conditions, SPP modes behave like a linear oscillator and will not directly contribute to the nonlinear response [16,22]. Instead, the  $X$  component of the polariton wave functions will cause a nonlinear response. Three different physical mechanisms may contribute to the transient nonlinearity. First, the creation of a finite  $X$  population may change the polariton amplitudes, without introducing a spectral shift. Since we observe an absorptive line shape in the linear reflectivity spectra [30], this exciton bleaching should lead to an absorptive spectrum, in stark contrast to the observed dispersive line shape in Fig. 2(b). We therefore conclude that this pump-induced bleaching of polariton resonances is weak. Second, the finite  $X$  population may reduce the net dipolar coupling between  $X$ s and SPPs and hence the mode splitting [16,22,25,50,51]. The pump-induced exciton creation results in a time-dependent normal mode splitting  $\Omega'_{\text{NMS}}(t) = \Omega_{\text{NMS}} \sqrt{n_0(t) - n_1(t)}$ , where  $\Omega_{\text{NMS}}$

is the normal mode splitting observed in the weak excitation limit and  $n_0$  and  $n_1$  are the  $X$  populations in the ground state ( $|0\rangle$ ) and excited state ( $|X\rangle$ ), respectively [16,22,30,52,53]. This reduction in  $\Omega'_{\text{NMS}}(t)$  has been shown to be dominant in recent studies of Rabi oscillation dynamics [16]. It results in a redshift of the UP and thus in a dispersive line shape with the opposite sign of that seen in Fig. 2(b). Finally, the off-resonant pump may transiently Stark shift the  $X$  resonance by an amount  $\Delta V(t)$ , effectively blueshifting both polariton resonances. The eigenfrequencies of the resulting, dressed polaritons can be obtained by diagonalizing an effective Hamiltonian for the  $X$ -SPP system in the presence of an off-resonant driving field [10,16]:

$$\tilde{\omega}_{\text{LP,UP}}(t) = \frac{[\tilde{\omega}_X + \Delta V(t) + \tilde{\omega}_P]}{2} \mp \frac{1}{2} \sqrt{[\tilde{\omega}_X + \Delta V(t) - \tilde{\omega}_P]^2 + \Omega'_{\text{NMS}}(t)^2}. \quad (2)$$

Hence, a pure OSE [ $\Omega'_{\text{NMS}}(t) = \Omega_{\text{NMS}}$ ] will result in a blueshift of both resonances. A pure reduction in  $\Omega_{\text{NMS}}$  [ $\Delta V(t) = 0$ ] will yield a blue- (red)shifted LP (UP). In Figs. 2(b) and 2(c), since we observe a clearly symmetric dispersive line shape, the change in polariton amplitude due to  $X$  saturation is obviously weak. We also see  $\Delta R < 0$  at  $\omega_{\text{pr}} > \omega_{\text{UP}}$ , reflecting a blueshifted UP. Therefore, from the  $\Delta R/R$  line shape and its occurrence only during pulse overlap, we can directly conclude that the transient signals reflect a pump-induced OSE of the UP mode. To our knowledge, this is the first observation of an OSE in a strongly coupled  $X$ -SPP system.

To get more quantitative microscopic insight into the polariton dynamics, we have solved OBEs for the hybrid nanostructure [30]. We assume a model Hamiltonian  $H = H_0 + H_R + H_{\text{LX}} + H_{\text{LP}}$ , where  $H_0$  is the free particle Hamiltonian for the  $X$  and SPP,  $H_R$  represents the  $X$ -SPP dipole interaction governed by  $\Omega_{\text{NMS}}$ , and  $H_{\text{LX}}$  ( $H_{\text{LP}}$ ) is the interaction between the incident laser field and the  $X$  (SPP). The radiative SPP lifetime is assumed to be  $\sim 10$  fs [48,54]. In the simulations, we have also phenomenologically included the transient reduction in normal mode splitting  $\Omega'_{\text{NMS}}(t)$  [8,16,22,30].

The simulated and observed  $\Delta R/R$  spectra at selected delays are compared in Fig. 2(c). The simulations qualitatively reproduce the experimental data and indicate a dispersive line shape arising from a blueshifted UP. Also, a pronounced nonlinearity seen only during the pump pulse confirm that, under these experimental conditions, the OSE is indeed the dominant nonlinearity. They indicate a maximum blueshift  $\Delta V_{\text{UP}} \sim 5$  meV, comparing well with blueshifts [Fig. 2(d)] deduced from an analysis of the experimental spectra with a Lorentzian oscillator model [22,30,49]. The OSE simulations also allow us to estimate the  $X$  and SPP population dynamics, which acquire finite



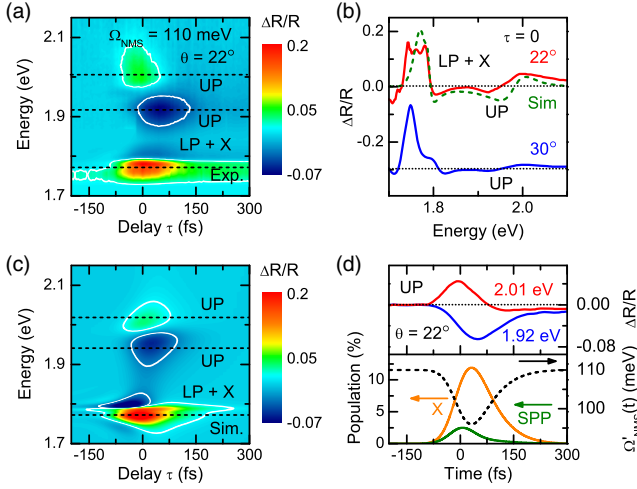


FIG. 3 (color online). (a)  $\Delta R/R(\tau, \omega_{pr})$  map of a  $J$ -aggregate–metal hybrid nanostructure with  $\Omega_{\text{NMS}} = 110$  meV measured at  $\theta = 22^\circ$ , detuned from the anticrossing. The transient dispersive signal at the UP (1.9–2.1 eV) shows a sign reversal with respect to that in Fig. 2(b). (b) Experimental (solid lines)  $\Delta R/R$  spectra ( $\tau = 0$ ) at two angles. The simulated spectrum (dashed line) at  $\theta = 22^\circ$  is also shown. (c) Simulated  $\Delta R/R(\tau, \omega_{pr})$  map including the effects of a time-dependent normal mode splitting  $\Omega'_{\text{NMS}}(t)$ . Dashed lines mark the maxima in  $\Delta R/R(\tau)$ . (d) Top: experimental  $\Delta R/R(\tau)$  at selected probe frequencies. Bottom: simulated pump-induced  $X$  and SPP population dynamics at  $\theta = 22^\circ$ .  $\Omega'_{\text{NMS}}(t)$  is also depicted (dashed line).

values only during the pulse overlap [Fig. 2(d)], indicating sufficiently weak spectral overlap between the pump and the LP resonance and a negligible long-lived incoherent  $X$  population. Effectively, coherent polarizations driven by the off-resonant pump destructively interfere at the end of the pulse. The observed nonlinearity is thus fully originating from coherent, transient populations existing only during the pulse. The pump-induced SPP population is weak due to the large detuning between the pump frequency and the SPP resonance.

To explore the effect of  $\Omega_{\text{NMS}}$  on the OSE and coherent population dynamics, we investigated a sample with higher  $\Omega_{\text{NMS}} = 110$  meV. The recorded  $\Delta R/R(\tau, \omega_{pr})$  for  $\theta = 22^\circ$  is shown in Fig. 3(a). Detuning from the anticrossing at  $\theta = 35^\circ$  is chosen to increase the UP amplitude in  $R_0(\omega_{pr})$  [30]. As can be seen in Fig. 3(a), a nonlinear response at the polariton resonances is again mainly observed during the pulse overlap. Interestingly, the sign of the dispersive UP line shape is now reversed compared to that seen at the LP resonance and also to that for a UP resonance in the hybrid nanostructure with smaller  $\Omega_{\text{NMS}}$  [Fig. 2(b)]. This sign reversal indicates that, instead of a blueshift of the UP resonance, we observe a redshift. The measurements repeated [30] for several incidence angles between  $20^\circ$ – $30^\circ$  yielded a transiently redshifted UP at all angles [Fig. 3(b)]. A similar sign reversal of the OSE has been reported before in semiconductor nanostructures, attributed

to  $XX$  formation [55], many-body interactions [12,56], and higher order Coulomb correlations [13].

In our case, Eq. (2) suggests that the physical mechanism responsible for the redshifted UP may be a transient reduction in  $\Omega'_{\text{NMS}}(t)$  induced by the coherently generated  $X$  population, in agreement with conclusions drawn in Ref. [16]. Yet, it is known from other material systems, specifically inorganic semiconductor microcavities with larger Bohr radii, that also other physical mechanisms such as pump-induced Coulomb interactions [52], changes in the  $X$  dephasing rate [57], alterations of the disorder potential [58], and polariton thermalization [53] may contribute to the transient reduction in  $\Omega'_{\text{NMS}}(t)$ , and hence to the OSE. Careful density dependent studies of the polariton dispersion [58] may provide important additional insight into the effects of such interactions on polariton excitations in hybrid organic systems. To support our assertion, we again resort to OBEs simulations including  $\Omega'_{\text{NMS}}(t)$ . The simulated  $\Delta R/R(\tau, \omega_{pr})$  map shown in Fig. 3(c) convincingly matches the experimental observations. As in the experiment, it predicts a pronounced nonlinearity only during the pump pulse. Figure 3(c) shows a red- (blue)shifted UP (LP) resonance, matching the observed sign reversal of the OSE. The measured ultrafast  $\Delta R$  dynamics shown in Fig. 3(d) clearly supports the coherent nature of the optical nonlinearity and the simulated population dynamics. From the simulations, we can now deduce information on both the OSE induced blueshift  $\Delta V_{\text{UP}}(t)$  and the coherent, transient reduction in  $\Omega'_{\text{NMS}}(t)$ . Under our experimental conditions,  $\Delta V(t)_{\text{UP}} \sim 5$  meV. As seen in Fig. 3(d) (dashed line), the transient reduction in  $\Omega'_{\text{NMS}}(t)$  by  $\sim 15$  meV largely overcompensates the Stark shift, effectively redshifting the UP. Here, the large decrease in  $\Omega'_{\text{NMS}}(t)$  in comparison to Figs. 2(b) and 2(c) is not primarily induced by an increase in the pump-induced  $X$  population  $n_1$  but rather by the largely enhanced  $\Omega_{\text{NMS}}$ .

Our results offer a very interesting approach for coherently controlling and enhancing OSEs in strongly coupled hybrid materials by transiently reducing  $\Omega'_{\text{NMS}}(t)$  rather than dressing  $X$  resonances [2,6,8–10]. It can greatly enhance OSEs to  $\sim 100$  meV in the ultrastrong coupling regime with  $\Omega_{\text{NMS}} \sim 700$  meV [23], making hybrid nanostructures interesting, not only for applications but also for exploring the underlying physics. Our experiments on large ensembles of  $X$ s have been performed with nanojoule pulse energies. We anticipate ultrafast coherent switching with femtojoule pulse energies for reduced sample area  $\leq 1 \mu\text{m}^2$ , even without considering plasmonic field enhancement.

In summary, we have presented the first experimental observation of OSEs in strongly coupled  $J$ -aggregate–metal hybrid nanostructures. For excitation with off-resonant ultrashort pump pulses, we observe fully coherent  $X$ -SPP optical nonlinearities. For systems with reduced  $\Omega_{\text{NMS}}$ , they reflect the expected transient dressing of the  $X$

resonances. For large  $\Omega_{\text{NMS}}$ , however, our results indicate a different type of response, greatly enhancing the OSE. It would be interesting to reduce the SPP mode volume and the coupled  $X$  number to reach the fundamental limits of ultrafast quantum plasmonics.

We thank the Deutsche Forschungsgemeinschaft (SPP 1391 and DFG-NSF Materials World Network), European Community (CRONOS, Grant No. 280879-2 and FP-7 INFRASTRUCTURES-2008-1, Laserlab Europe II, Contract No. 228334) and the Korea Foundation for International Cooperation of Science and Technology (Global Research Laboratory project, Project No. K20815000003) for financial support. G. C. acknowledges support by the European Community under Graphene Flagship (Contract No. CNECT-ICT-604391).

\*parinda@iitb.ac.in

†christoph.lienau@uni-oldenburg.de

- [1] B. R. Mollow, *Phys. Rev. A* **5**, 2217 (1972).
- [2] H. Häffner, S. Gulde, M. Riebe, G. Lancaster, C. Becher, J. Eschner, F. Schmidt-Kaler, and R. Blatt, *Phys. Rev. Lett.* **90**, 143602 (2003).
- [3] A. Wirth *et al.*, *Science* **334**, 195 (2011).
- [4] J. M. Pirkkalainen, S. U. Cho, J. Li, G. S. Paraoanu, P. J. Hakonen, and M. A. Sillanpaa, *Nature (London)* **494**, 211 (2013).
- [5] B. B. Buckley, G. D. Fuchs, L. C. Bassett, and D. D. Awschalom, *Science* **330**, 1212 (2010).
- [6] D. Fröhlich, A. Nöthe, and K. Reimann, *Phys. Rev. Lett.* **55**, 1335 (1985).
- [7] M. Saba, F. Quochi, C. Ciuti, D. Martin, J.-L. Staehli, B. Deveaud, A. Mura, and G. Bongiovanni, *Phys. Rev. B* **62**, R16322 (2000).
- [8] T. Unold, K. Mueller, C. Lienau, T. Elsaesser, and A. D. Wieck, *Phys. Rev. Lett.* **92**, 157401 (2004).
- [9] J. Zhang, Y. Tang, K. Lee, and M. Ouyang, *Nature (London)* **466**, 91 (2010).
- [10] A. Hayat, C. Lange, L. A. Rozema, A. Darabi, H. M. van Driel, A. M. Steinberg, B. Nelsen, D. W. Snoke, L. N. Pfeiffer, and K. W. West, *Phys. Rev. Lett.* **109**, 033605 (2012).
- [11] E. Cancellieri, A. Hayat, A. M. Steinberg, E. Giacobino, and A. Bramati, *Phys. Rev. Lett.* **112**, 053601 (2014).
- [12] C. Ell, J. F. Müller, K. El Sayed, and H. Haug, *Phys. Rev. Lett.* **62**, 304 (1989).
- [13] C. Sieh *et al.*, *Phys. Rev. Lett.* **82**, 3112 (1999).
- [14] T. Kobayashi, *J-aggregates* (World Scientific, Singapore, 1996).
- [15] F. Würthner, T. E. Kaiser, and C. R. Saha-Möller, *Angew. Chem., Int. Ed.* **50**, 3376 (2011).
- [16] See P. Vasa, W. Wang, R. Pomraenke, M. Lammers, M. Maiuri, C. Manzoni, G. Cerullo, and C. Lienau, *Nat. Photonics* **7**, 128 (2013) and supporting on-line material.
- [17] D. M. Coles, N. Somaschi, P. Michetti, C. Clark, P. G. Lagoudakis, P. G. Savvidis, and D. G. Lidzey, *Nat. Mater.* **13**, 712 (2014).
- [18] I. Pockrand, A. Brillante, and D. Moebius, *J. Chem. Phys.* **77**, 6289 (1982).
- [19] J. Bellessa, C. Bonnand, J. C. Plenet, and J. Mugnier, *Phys. Rev. Lett.* **93**, 036404 (2004).
- [20] J. Dintinger, S. Klein, F. Bustos, W. L. Barnes, and T. W. Ebbesen, *Phys. Rev. B* **71**, 035424 (2005).
- [21] N. T. Fofang, T. H. Park, O. Neumann, N. A. Mirin, P. Nordlander, and N. J. Halas, *Nano Lett.* **8**, 3481 (2008).
- [22] P. Vasa, R. Pomraenke, G. Cirmi, E. De Re, W. Wang, S. Schwieger, D. Leipold, E. Runge, G. Cerullo, and C. Lienau, *ACS Nano* **4**, 7559 (2010).
- [23] T. Schwartz, J. A. Hutchison, C. Genet, and T. W. Ebbesen, *Phys. Rev. Lett.* **106**, 196405 (2011).
- [24] W. Wang, P. Vasa, R. Pomraenke, R. Vogelgesang, A. de Sio, E. Sommer, M. Maiuri, C. Manzoni, G. Cerullo, and C. Lienau, *ACS Nano* **8**, 1056 (2014).
- [25] J. Dintinger, I. Robel, P. Kamat, C. Genet, and T. Ebbesen, *Adv. Mater.* **18**, 1645 (2006).
- [26] D. E. Chang, A. S. Sorensen, E. A. Demler, and M. D. Lukin, *Nat. Phys.* **3**, 807 (2007).
- [27] M. Kauranen and A. V. Zayats, *Nat. Photonics* **6**, 737 (2012).
- [28] R. F. Oulton, V. J. Sorger, T. Zentgraf, R. M. Ma, C. Gladden, L. Dai, G. Bartal, and X. Zhang, *Nature (London)* **461**, 629 (2009).
- [29] V. I. Klimov, S. A. Ivanov, J. Nanda, M. Achermann, I. Bezel, J. A. McGuire, and A. Piryatinski, *Nature (London)* **447**, 441 (2007).
- [30] See Supplemental Material at <http://link.aps.org/supplemental/10.1103/PhysRevLett.114.036802>, which includes Refs. [31–45], for information on experiments and simulations.
- [31] H. Fidder, J. Knoester, and D. A. Wiersma, *Chem. Phys. Lett.* **171**, 529 (1990).
- [32] K. G. Lee and Q. Han Park, *Phys. Rev. Lett.* **95**, 103902 (2005).
- [33] H. Fidder, J. Knoester, and D. A. Wiersma, *J. Chem. Phys.* **95**, 7880 (1991).
- [34] H. Fidder, J. Knoester, and D. A. Wiersma, *J. Chem. Phys.* **98**, 6564 (1993).
- [35] G. S. Agarwal, *Quantum Statistical Theories of Spontaneous Emission and their Relation to Other Approaches*, Quantum Optics Vol. 70 (Springer, New York, 1974).
- [36] M. O. Scully and M. S. Zubairy, *Quantum Optics* (Cambridge University Press, Cambridge, 2001).
- [37] D. F. Walls and G. J. Milburn, *Quantum Optics* (Springer, New York, 2008).
- [38] R. J. Thompson, G. Rempe, and H. J. Kimble, *Phys. Rev. Lett.* **68**, 1132 (1992).
- [39] C. Weisbuch, M. Nishioka, A. Ishikawa, and Y. Arakawa, *Phys. Rev. Lett.* **69**, 3314 (1992).
- [40] J. P. Reithmaier, G. Sk, A. Löffler, C. Hofmann, S. Kuhn, S. Reitzenstein, L. V. Keldysh, V. D. Kulakovskii, T. L. Reinecke, and A. Forchel, *Nature (London)* **432**, 197 (2004).
- [41] T. Yoshie, A. Scherer, J. Hendrickson, G. Khitrova, H. M. Gibbs, G. Rupper, C. Ell, O. B. Shchekin, and D. G. Deppe, *Nature (London)* **432**, 200 (2004).
- [42] G. Lindblad, *Commun. Math. Phys.* **48**, 119 (1976).

- [43] H. Haug and S. W. Koch, *Quantum Theory of the Optical and Electronic Properties of Semiconductors*, 4th ed. (World Scientific, Singapore, 2005).
- [44] E. T. Jaynes and F. W. Cummings, *Proc. IEEE* **51**, 89 (1963).
- [45] G. Khitrova, H. M. Gibbs, F. Jahnke, M. Kira, and S. W. Koch, *Rev. Mod. Phys.* **71**, 1591 (1999).
- [46] C. Manzoni, D. Polli, and G. Cerullo, *Rev. Sci. Instrum.* **77**, 023103 (2006).
- [47] P. Vasa *et al.*, *Phys. Rev. Lett.* **101**, 116801 (2008).
- [48] C. Ropers, D. J. Park, G. Stibenz, G. Steinmeyer, J. Kim, D. S. Kim, and C. Lienau, *Phys. Rev. Lett.* **94**, 113901 (2005).
- [49] W. Wang, P. Vasa, E. Sommer, A. de Sio, P. Gross, R. Vogelgesang, and C. Lienau, *J. Opt.* **16**, 114021 (2014).
- [50] R. Houdré, J. L. Gibernon, P. Pellandini, R. P. Stanley, U. Oesterle, C. Weisbuch, J. O’Gorman, B. Roycroft, and M. Ilegems, *Phys. Rev. B* **52**, 7810 (1995).
- [51] A. Tredicucci, Y. Chen, V. Pellegrini, M. Börger, and F. Bassani, *Phys. Rev. A* **54**, 3493 (1996).
- [52] G. Rossbach, J. Levrat, E. Felton, J.-F. Carlin, R. Butté, and N. Grandjean, *Phys. Rev. B* **88**, 165312 (2013).
- [53] S. R. K. Rodriguez, J. Feist, M. A. Verschuuren, F. J. Garcia Vidal, and J. Gómez Rivas, *Phys. Rev. Lett.* **111**, 166802 (2013).
- [54] D. S. Kim, S. Hohng, V. Malyarchuk, Y. Yoon, Y. Ahn, K. Yee, J. Park, J. Kim, Q. Park, and C. Lienau, *Phys. Rev. Lett.* **91**, 143901 (2003).
- [55] M. Combescot and R. Combescot, *Phys. Rev. Lett.* **61**, 117 (1988).
- [56] W. H. Knox, D. S. Chemla, D. A. B. Miller, J. B. Stark, and S. Schmitt-Rink, *Phys. Rev. Lett.* **62**, 1189 (1989).
- [57] F. Jahnke *et al.*, *Phys. Rev. Lett.* **77**, 5257 (1996).
- [58] J. Kasprzak *et al.*, *Nature (London)* **443**, 409 (2006).